# Reduced-order model for the non-linear dynamics of cables

Charlélie Bertrand, Alireza Ture Savadkoohi, Vincent Acary, Claude-Henri Lamarque

# Reduced-order model for the non-linear dynamics of cables

Charlelie Bertrand *, Alireza Ture Savadkoohi†, Vincent Acary‡, Claude-Henri Lamarque§

September 2021

**Abstract**

Formulation of governing equations for an elastic cable have a long and dated history. A unified framework to detect the dynamics of such systems is detailed, justified and assessed numerically. Modal analyses are performed in the Frenet basis which parts the motion into the local frame and accounts accurately for the system's physics. In this article, a methodology to produce arbitrary reduced-order models for cable nonlinear dynamics is provided. The results obtained from the latter via direct time integration are challenged numerically via a comparison with results of nonlinear finite element method.

**Keywords:** Cable Mechanics, Modal analysis, Nonlinear Dynamics, Arc-length Continuation, Frequency Responses, Finite Element

# Introduction

The statics of cable have been investigated thoroughly in the past [14, 18, 28, 29]. The exact nonlinear geometry taken by a cable subjected to its self-weight and pinned at both ends is called the catenary. The parabolic approximation have been used for a long time in engineering applications depending on the sag-to-span ratio [20, 24]:

- The cable exhibits large deflection (i.e. span depth ratio $> \frac{1}{8}$) or inclined supports: the exact solution must be used

*Corresponding author - Univ Lyon, ENTPE, LTDS UMR CNRS 5513, Rue Maurice Audin 69518 Vaulx-en-Velin Cedex, France
†Univ Lyon, ENTPE, LTDS UMR CNRS 5513, Rue Maurice Audin 69518 Vaulx-en-Velin Cedex, France
‡Univ. Grenoble Alpes, INRIA, CNRS, Grenoble INP, LJK, 38000 Grenoble, France
§Univ Lyon, ENTPE, LTDS UMR CNRS 5513, Rue Maurice Audin 69518 Vaulx-en-Velin Cedex, France

- The cable exhibits small deflection (i.e. span depth ratio $< \frac{1}{8}$) and aligned supports: the parabolic approximation can be used

Investigations about frequencies and modes for the cable with various assumptions and applications followed the question of the statics. For instance for an inelastic cable [44], for an inelastic cable with an heterogeneous mass distribution [45], for a suspended chain plus experimental check [36] or for a pure catenary [46]. However, a lot of earlier works were not valid for the taut string [21] until the works of Soler [50] and Simpson [47] where the oscillations are investigated as a dynamic perturbation of a steady-state regime. For bridges, various methods have been proposed for the evaluation of cable frequencies [16, 22, 37].

One of the most notable contributions is the one of Irvine and Caughey [19, 20] who unified all known developments and clarified the transition from the sagged elastic cable frequencies towards the vibrating string frequencies accompanied with experimental validation. An elasto-geometric parameter given in [20] is now denoted as Irvine's parameter:

$$\lambda_{\text{Irv}}^2 = \left(\frac{\mu g d}{H}\right)^2 \frac{EA}{H \int_0^L \cos(\theta(S))^3 \mathrm{d}S} \tag{1}$$

where $\mu$ is linear density of the cable, $g$ is the gravity constant, $d$ the horizontal span distance between two supports, $H$ the horizontal constant component of the tension, $EA$ is the rigidity of the cable, $L$ the length of the cable and $\theta$ gives the angle between the horizontal and the cable axial direction.

The cable exhibits families of modes and their symmetric or anti-symmetric nature have been investigated and shown to be a function of the Irvine's parameter. More developments according to the inclination of the rest position have been done which extended the results of Irvine to more sophisticated situations via introducing new geometric parameters [52, 55].

Until the early eighties, only the linear dynamics of cables were treated. At the author knowledge, the first work tracing a nonlinear response is from Hagedorn and Schäfer [17]. Their approach is a milestone for the nonlinear dynamics of cables as they introduced the combined use of Ritz-Galerkin and perturbation methods to treat the nonlinear terms in the original system equations. This approach results in condensing the dynamics on some selected modes. Global methodology consists in using a polynomial expansion of system variables, then a decomposition of the displacement along some modes is assumed. The resulting equation or their multiple dimension equivalents have been studied for the last forty years

$$\ddot{q} + \mu\dot{q} + q + c_2 q^2 + c_3 q^3 = f(t) \tag{2}$$

where $q$ is a modal coordinate and $f$ is an arbitrary external force vector. The biggest advantage is to provide with

equations that can be investigated numerically, providing some design tools.

The work of Luongo et al. [30] dealt with a two degree-of-freedom (dof) model for an elastic cable taking into account all geometrical nonlinearities. They describe the influence of the cubic and quadratic nonlinearities on the frequencies of the cable. Complementary studies about the effect of nonlinearities have been lead by Rega et al. [43] and investigated further two years later by Luongo et al. [31]. Benedettini et al. [6] showed that the cable exhibits strong coupled oscillations and that exchanges between the first and second mode are stronger when the cable sag increases. In addition to that, Benedettini and Rega [3] highlighted a notable difference between the cable and the string: a cable exhibits softening-hardening behavior contrary to a string and also that subharmonic resonances explains some rich dynamical responses [41].

The nonlinear dynamics of cable entail a wide range of scenario including chaotic responses [53] or modes resonances [26, 35] depending on the solicitation or the geometry considered. Several works are focused on all the zoology of the cable nonlinear responses [4, 5, 27, 38, 40] with in-depth comparisons between models containing different number of dofs or different nature of modes.

The review of Rega [39] is quite extensive about all the phenomenon possible in cable dynamics, both numerically and experimentally. Meanwhile, nonlinear dynamics of inclined cables continued to be investigated for example by Berlioz and Lamarque [7] who provided a two dof model for an inclined cable and its treatment via the method of multiple scales to obtain the cable response in resonant regimes with comparisons with experiments. A model for the nonlinear vibrations of an inclined cable treated by finite differences and supplemented by experiments was given in the joined work of Srinil and Rega[42]. Meanwhile, cable dynamics with point loads and point solicitations are treated in the works of Sofi and Muscolino [48, 49] where a model for an inclined cable carrying moving oscillators is proposed.

A lot of modeling aspects for cable have been collected, investigated and precised by Lacarbonara and Pacitti [25] who model cable with flexural stiffness and a visco-elastic constitutive law. This work emphasized on the non-compression condition inherent to the cable equilibrium. The same modeling context was chosen by Arena who to study the nonlinear vibrations of a cable derived from Cosserat theory [2] which add the torsional stiffness in consideration. Other models have been proposed in the literature as for example the one of Pai and Nayfeh [33] where Poisson effect were considered.

Investigation about transient regimes for a cable carrying moving masses have been done by Wang and Rega [23] and they discussed about adaption of the condensed model for non-shallow cables. Recently, Warminski et al. [54] revisited in details the four dof model of Benedettini [6] dating back to 1995 and made considerable efforts to derive a rich zoology of cable behaviors. They exhibits multiple resonances and primary resonance and improved the stability analysis done previously for this cable model.

Current considerations in nonlinear vibration of cables are the galloping phenomenon in shallow cables (e.g see work of Ferretti [12]) or also complex structures where a cable is bounded to two other structural elements for example the beam-cable-beam structure studied by Gatulli et al. [15]. Our motivation with this paper is to provide a uniform framework to derive the system governing equations and to depict every single assumptions that lead to characterize the frequencies and modes of the system. Eventually the nonlinear dynamics of a cable will be treated via formulating a reduced-order-model (ROM) via a Ritz-Galerkin procedure that trace longitudinal, normal and transversal motion accurately. The reliability will be investigated via comparisons with nonlinear finite element method (FEM) which has been poorly investigated until now.

This work aims to highlight that the cable nonlinear dynamics for large displacements require careful numerical applications. The use of ROM should be justified to avoid wrong displacement estimation. The combined use of FEM and ROM is therefore suitable to assess for the validity of an approach. The main results presented here are the global methodology to derive an arbitrary ROM for cable dynamics. Its validity is challenged numerically via a comparison to computations made with FEM. It is shown that there is a qualitative agreement between the approach but quantitative agreement are hardly met for large displacements applications. Our work is organized as it follows: Section  system of interest and the particular case of a cable subjected to its self-weight only. Section  deals with the modal analysis of cables with an analytical point of view (assumptions are given explicitly) and also with a purely numerical point of view via finite difference method. Section 22 depicts a general methodology to build ROMs for cable systems and applications that derive from it. For this model, the longitudinal displacement is not discarded and kept to build a ROM. Section 22 sums up our contributions and opens the debate about the treatment of the nonlinear dynamics of a cable via the coupled used of reduced-order models and nonlinear finite element dynamics. A fair assessment of the reliability of the ROM is given according to a comparison with FEM.

# Equilibrium of a three-dimensional cable

In this section, the assumptions for the system of interest are presented. The equations for the steady-state are presented and treated for the case of a vertical and uniform load. Finally, the perturbed dynamics of a cable subjected to a general load is presented.

## Curvilinear domains

The cable model has its origin in the curvilinear domain mechanics [1, 32, 34]. The domain is described in its current configuration, sometimes denoted as "studied", "stretched" or "Eulerian" configuration. The particles composing the

domain will be part of the Cartesian space $\mathbb{R}^3$ with the basis $(O, \mathbf{x}, \mathbf{y}, \mathbf{z})$ and we have

$$\mathbf{R}(S,t) = x(S,t)\,\mathbf{x} + y(S,t)\,\mathbf{y} + z(S,t)\,\mathbf{z} \tag{3}$$

The main property of a curvilinear domain is to be a parametrized curve, then an arc-length variable, $S$, will be used for the spatial dependency of all system variables. In another words, the function

$$(S,t) \longrightarrow \mathbf{R}(S,t) \tag{4}$$

allows parameterize every particles of the domain and defines its orientation at a given time $t$. That is to say, the bigger $S$ is, the further we are on the frame. This function is generally defined on an open segment i.e. $S \subset ]0, L[$. The curvilinear abscissa, $S$, defines an orientation in the sense that a tangent vector can be defined

$$\mathbf{d}_1(S,t) = \frac{\mathbf{R}'(S,t)}{\|\mathbf{R}'(S,t)\|} \tag{5}$$

where $\bullet'$ denotes the differentiation with respect to $S$.

The existence of $\mathbf{d}_1(S,t)$ requires that we have

$$\|\mathbf{R}'(S,t)\| \neq 0 \quad \forall\, 0 \leqslant S \leqslant L\ ,\ \forall t \geqslant 0 \tag{6}$$

An orthogonal counterpart of $\mathbf{d}_1(S,t)$ is given by $\mathbf{d}_2(S,t)$ and coined as the normal vector. The latter belongs to the $(\mathbf{x}, \mathbf{y})$-plane and is computed as

$$\mathbf{d}_2(S,t) = \mathbf{z} \wedge \mathbf{d}_1(S,t) \tag{7}$$

where $\wedge$ stands for the wedge product.

The triplet $(\mathbf{d}_1(S,t), \mathbf{d}_2(S,t), \mathbf{z})$ is coined as the Frenet basis. It corresponds to the unit-orthogonal right-handed local frame attached to every cable particle.

## System of interest

We are interested into the equilibrium of a cable with unstretched length $L$ which spans between $\mathbf{R}_0$ and $\mathbf{R}_L$. The cable is assumed to be uniform i.e. is linear density $\rho$ and its rigidity $EA$ are constant along all the span. An initial tension, $T_0$ is enforced in $\mathbf{R}_0$ and the cable lies in the gravitational field given by $g$. Moreover we assume that there is no point load applied to the cable. Due to the geometry of the system and the gravitational field taken along $\mathbf{y}$, we

can assume that the steady-state lies into the plane given by $z = 0$. Moreover, with a suitable translation we can assume without loss of generality that

$$\mathbf{R}_0 = \begin{bmatrix} 0 \\ 0 \\ 0 \end{bmatrix} \quad ; \quad \mathbf{R}_L = \begin{bmatrix} d \\ h \\ 0 \end{bmatrix} \quad ; \quad \mathbf{R}(S,t) = \begin{bmatrix} x(S,t) \\ y(S,t) \\ z(S,t) \end{bmatrix} \tag{8}$$

An arc-length coordinate, $S$, is used to locate cable particles' positions, $\mathbf{R}(S,t)$, in the Cartesian space.
The cable is assumed to be perfectly flexible, therefore it cannot resist to any moment or torque. Only its internal tensile force ensures the balance of forces. The latter is given by the product of a positive scalar quantity called tension, $T$, and the axial vector. Moreover the cable is linear elastic and all geometrical nonlinearities are kept, then

$$T(S,t) = EA\left(\|\mathbf{R}(S,t)\| - 1\right) \geqslant 0 \tag{9}$$

For the sake of conciseness, $S$ and $t$ dependencies will be removed from system equations. Considering that damping, referred as $\mu$, might be added in the sequel, the full dynamics of such a system are given by

$$\rho\ddot{\mathbf{R}} + 2\mu\dot{\mathbf{R}} = EA\left((\|\mathbf{R}'\| - 1)\frac{\mathbf{R}'}{\|\mathbf{R}'\|}\right)' + \mathbf{b} \tag{10}$$

where $\dot{\bullet}$ stands for the time differentiation. The system of interest is depicted in Figure 1.

## Equilibrium in the case of a vertical and uniform load

In this section, we are interested in treating the static equilibrium of a hanging cable. Due to the case studied, the cable is contained into the $(\mathbf{x}, \mathbf{y})$-plane. The positions and the axial vector associated to this equilibrium are denoted by $\mathbf{r}$ and $\mathbf{e}$ respectively. The distributed load $\mathbf{b}$ is considered to be only the self-weight. The equilibrium reads

$$EA\left[(\|\mathbf{r}'\| - 1)\mathbf{e}\right]' - g\mathbf{y} = \mathbf{0} \tag{11}$$

In other words, the static elastic forces, $f_e(\mathbf{r})$ given by

$$f_e(\mathbf{r}) = EA\left[(\|\mathbf{r}'\| - 1)\frac{\mathbf{r}'}{\|\mathbf{r}'\|}\right] \tag{12}$$

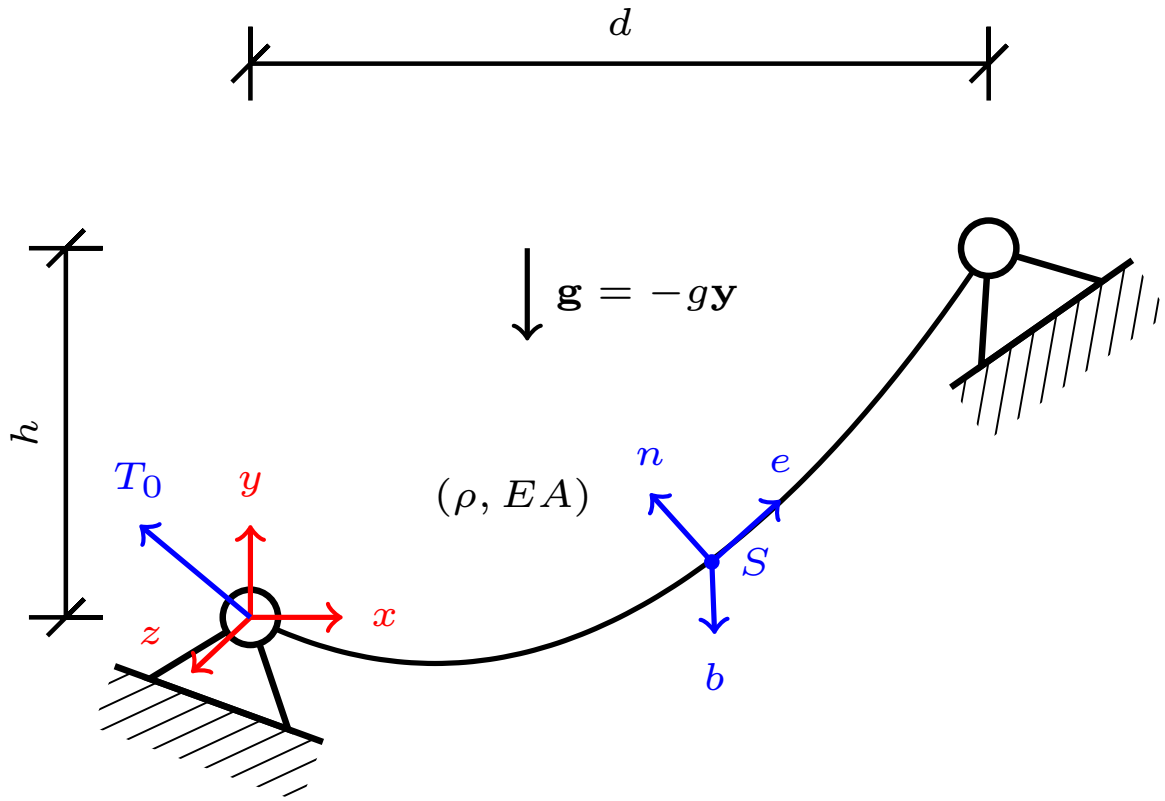


Figure 1: Elastic cable hanging between two supports in the gravitational field $\mathbf{g} = -g\mathbf{y}$ with initial tension $T_0$ and the Frenet basis $(\mathbf{e}(S), \mathbf{n}(S), \mathbf{z})$

are balancing the self-weight of the cable. A first integration between 0 and $S$, $0 \leqslant S \leqslant L$, yields

$$EA\left(\|\mathbf{r}'\| - 1\right)\mathbf{e} = \frac{T_0}{\sqrt{1+\eta^2}}\begin{bmatrix}1\\ \eta\end{bmatrix} + \begin{bmatrix}0\\ \rho g S\end{bmatrix} \tag{13}$$

where the initial unit axial vector, $\mathbf{e}(0)$, is parameterized with one parameter $\eta$ as follows

$$\mathbf{e}(0) = \frac{1}{\sqrt{1+\eta^2}}\begin{bmatrix}1\\ \eta\end{bmatrix} \tag{14}$$

and the initial value of tension is given by $T_0$. As a consequence, following equality is obtained due to the unit property of $\mathbf{e}$

$$T = \frac{T_0}{\sqrt{1+\eta^2}}\sqrt{1 + \left(\eta + \frac{\rho g\sqrt{1+\eta^2}}{T_0}\right)^2} \tag{15}$$

and

$$\mathbf{e} = \frac{1}{\sqrt{1 + \left(\eta + \frac{\rho g\sqrt{1+\eta^2}}{T_0}\right)^2}}\begin{bmatrix}1\\ \eta + \frac{\rho g\sqrt{1+\eta^2}}{T_0}\end{bmatrix} \tag{16}$$

Combining (13-16) and using the fact that $\mathbf{e}$ is unit, we obtain that

$$\mathbf{r}' = \|\mathbf{r}'\|\mathbf{e} = \left(\frac{T}{EA} - 1\right)\mathbf{e} \tag{17}$$

The latter can be integrated between $S \in [0, 1]$ and 1, which yields

$$d - x = \frac{T_0(L-S)}{EA\sqrt{1+\eta^2}} + T_0\frac{\sinh^{-1}(\eta + \frac{\rho g\sqrt{1+\eta^2}}{T_0}L) - \sinh^{-1}(\eta + \frac{\rho g\sqrt{1+\eta^2}}{T_0}S)}{\rho g\sqrt{1+\eta^2}} \tag{18}$$

$$\begin{aligned} h - y =& \frac{\eta T_0(L-S)}{EA\sqrt{1+\eta^2}} + \rho g\frac{L^2 - S^2}{2EA} \\ &+ T_0\frac{\sqrt{1+\left(\eta + \frac{\rho g\sqrt{1+\eta^2}}{T_0}L\right)^2} - \sqrt{1+\left(\eta + \frac{\rho g\sqrt{1+\eta^2}}{T_0}S\right)^2}}{\rho g\sqrt{1+\eta^2}} \end{aligned} \tag{19}$$

These developments are valid under the assumption that the strain is positive which is ensured by the physics of the hauling rope. If the assumption is not satisfied, derivations have to be done differently.

The profiles given by (18) and (19) can be evaluated into $S = 0$, which provide a set of two coupled nonlinear equations

$$\begin{cases} d = \dfrac{T_0 L}{EA\sqrt{1+\eta^2}} + T_0\dfrac{\sinh^{-1}(\eta + \frac{\rho g\sqrt{1+\eta^2}}{T_0}L) - \sinh^{-1}(\eta)}{\rho g\sqrt{1+\eta^2}} \\ h = \dfrac{\eta T_0 L}{EA\sqrt{1+\eta^2}} + \rho g\dfrac{L^2}{2EA} + T_0\dfrac{\sqrt{1+\left(\eta + \frac{\rho g\sqrt{1+\eta^2}}{T_0}L\right)^2} - \sqrt{1+\eta^2}}{\rho g\sqrt{1+\eta^2}} \end{cases} \tag{20}$$

The latter is often left ambiguous in the work related to cable since its resolution depends on the domain considered. Indeed we have to choose whether the unknown is the couple $(T_0, \eta)$ or the couple $(L, \eta)$. Moreover, we can also choose to work with the horizontal component of the cable internal forces instead of the tension.

Once (20) is solved, the modal content can be computed.

# Tracing modal content of the system

The goal of this section is to present the equations that lead to frequency tracing. Modes are an essential tool to build reliable basis for Ritz-Galerkin procedures for instance. This subject is treated under various cases and assumptions in the literature. In order to give a different vision, we propose here a Frenet basis vision of the dynamics which sums up all contributions made in analytical developments in the domain of cable frequencies.

## Equations for the small vibrations

The governing equations given in (10) in the case of a vertical and uniform load is considered with a small vibration $\mathbf{u}$ around the static equilibrium given by $\mathbf{r}$. Meaning that

$$\mathbf{R} = \mathbf{r} + \mathbf{u} \tag{21}$$

It follows that

$$\dot{\mathbf{R}} = \dot{\mathbf{u}} \quad , \quad \ddot{\mathbf{R}} = \ddot{\mathbf{u}} \tag{22}$$

The actual tangent vector is obtained with a first order Taylor expansion

$$\frac{\mathbf{R}'}{\|\mathbf{R}'\|} = \frac{\mathbf{r}' + \mathbf{u}'}{\|\mathbf{r}' + \mathbf{u}'\|} \approx \frac{\mathbf{r}'}{\|\mathbf{r}'\|} + \frac{\mathbf{u}'}{\|\mathbf{r}'\|} - \frac{(\mathbf{r}' \cdot \mathbf{u}')}{\|\mathbf{r}'\|^3}\mathbf{r}' \tag{23}$$

$$= \mathbf{e} + \frac{1}{\|\mathbf{r}'\|}\left(\mathbf{u}' - (\mathbf{e} \cdot \mathbf{u}')\mathbf{e}\right) \tag{24}$$

where $\mathbf{r}$ is given by (11). The actual strain is obtained the same way as

$$\|\mathbf{R}'\| - 1 = \|\mathbf{r}' + \mathbf{u}'\| - 1 \approx \|\mathbf{r}'\| - 1 + (\mathbf{e} \cdot \mathbf{u}') \tag{25}$$

Once (24) and (25) are injected into (10), the linearized dynamics are obtained considering only the first order terms in $\mathbf{u}$

$$\rho\ddot{\mathbf{u}} = EA\left[\frac{\|\mathbf{r}'\| - 1}{\|\mathbf{r}'\|}\mathbf{u}' + \frac{\mathbf{e} \cdot \mathbf{u}'}{\|\mathbf{r}'\|}\mathbf{e}\right]' \tag{26}$$

where non constant coefficients are obtained from the static equilibrium and statics given by (11) allows to simplify (10). These equations are more amenable when formulated into the local frame (Frenet basis). In another words, the vibrations is decomposed as follows

$$\mathbf{u} = p\,\mathbf{e} + q\,\mathbf{n} + b\,\mathbf{z} \tag{27}$$

where the triads $(\mathbf{e}, \mathbf{n}, \mathbf{z})$ is the unit-orthogonal local frame obtained from the steady-state configuration (visible in Figure 1). The expressions of both axial and normal vectors are

$$\mathbf{e} = \frac{1}{\sqrt{1 + \left(\eta + \frac{\rho g \sqrt{1+\eta^2}}{T_0}\right)^2}} \begin{bmatrix} 1 \\ \eta + \frac{\rho g \sqrt{1+\eta^2}}{T_0} \end{bmatrix} \tag{28}$$

$$\mathbf{n} = \mathbf{z} \wedge \mathbf{e} = -\frac{1}{\sqrt{1 + \left(\eta + \frac{\rho g \sqrt{1+\eta^2}}{T_0}\right)^2}} \begin{bmatrix} \eta + \frac{\rho g \sqrt{1+\eta^2}}{T_0} \\ -1 \end{bmatrix} \tag{29}$$

The following properties arise from this local frame is obtained via differentiation

$$\mathbf{e}' = \mathcal{K}\mathbf{n} \quad , \quad \mathbf{n}' = -\mathcal{K}\mathbf{e} \quad , \quad \mathbf{z}' = 0 \tag{30}$$

where we used the following notation for the curvature of the cable

$$\mathcal{K} = \frac{\frac{\rho g}{T_0}\sqrt{1+\eta^2}}{1 + \left(\eta + \frac{\rho g}{T_0}\sqrt{1+\eta^2} S\right)^2} \tag{31}$$

Then the derivatives of the vibration reads

$$\dot{\mathbf{u}} = \dot{p}\,\mathbf{e} + \dot{q}\,\mathbf{n} + \dot{b}\,\mathbf{z} \tag{32}$$

$$\ddot{\mathbf{u}} = \ddot{p}\,\mathbf{e} + \ddot{q}\,\mathbf{n} + \ddot{b}\,\mathbf{z} \tag{33}$$

$$\mathbf{u}' = \left(p' - \mathcal{K}q\right)\,\mathbf{e} + \left(q' + \mathcal{K}p\right)\,\mathbf{n} + b'\,\mathbf{z} \tag{34}$$

$$\mathbf{u}'' = \left[\left(p' - \mathcal{K}q\right)' - \mathcal{K}\left(q' + \mathcal{K}p\right)\right]\,\mathbf{e} + \left[\left(q' + \mathcal{K}p\right)' + \mathcal{K}\left(p' - \mathcal{K}q\right)\right]\,\mathbf{n} + b''\,\mathbf{z} \tag{35}$$

The later derivations can be injected into (26) which provides in a compact manner

$$\rho\,\ddot{p} = EA\,\left[\left(p' - \mathcal{K}q\right)' - \frac{\|\mathbf{r}'\| - 1}{\|\mathbf{r}'\|}\mathcal{K}\left(q' + \mathcal{K}p\right)\right] \tag{36}$$

$$\rho\,\ddot{q} = EA\,\left[\left(\frac{\|\mathbf{r}'\| - 1}{\|\mathbf{r}'\|}\left(q' + \mathcal{K}p\right)\right)' + \mathcal{K}\left(p' - \mathcal{K}q\right)\right] \tag{37}$$

$$\rho\,\ddot{b} = EA\,\left[\frac{\|\mathbf{r}'\| - 1}{\|\mathbf{r}'\|}b'\right]' \tag{38}$$

Equations (36)-(38) can be treated can be treated numerically or analytically which is the topic of the next section.

# Approximate analytic treatment of the cable vibrations

The theory of linear free vibrations of cable is quite extensive and has been extensively treated in the literature. Here we give the extensive set of assumptions that leads to equations for cable frequencies and modes.
It is shown that those modes are not orthogonal in the general case which is obscured in the literature by the fact that longitudinal dynamics are discarded in linear and nonlinear analysis.

## Out of plane small vibrations

We first focus on (38) that governs the transverse displacement. This kind of motion is a modified pendulum motion. The reader may imagine the bouncing of a hammock suspended between two trees as an illustration for these motions. Let us assume that the transverse displacement is given by

$$b = B(S)e^{i\omega t} \quad ; \quad i^2 = -1 \tag{39}$$

A substitution of (39) into (38) and yields

$$\rho\omega^2 B + EA\left[\frac{\|\mathbf{r}'\| - 1}{\|\mathbf{r}'\|}B'\right]' = 0 \tag{40}$$

It appears from the numerical computation that the following quantity $\frac{\|\mathbf{r}'\|-1}{\|\mathbf{r}'\|}$ is almost constant along the cable for high values of $EA$ (which is often true in reality) such that its derivative might be neglected in first approach. It results in the following differential equation

$$\rho\omega^2 B + \alpha^2 B'' = 0 \quad ; \quad \alpha^2 = EA\,\frac{\|\mathbf{r}'\| - 1}{\|\mathbf{r}'\|} \tag{41}$$

The latter admits as solution

$$B = b_1 \cos\left(\sqrt{\rho}\frac{\omega}{\alpha}S\right) + b_2 \sin\left(\sqrt{\rho}\frac{\omega}{\alpha}S\right) \tag{42}$$

With the boundary conditions, constants $b_1$ and $b_2$ are found and the frequencies are obtained as

$$\sin\left(\sqrt{\rho}\frac{\omega}{\alpha}L\right) = 0 \iff \omega = k\frac{\alpha\pi}{\sqrt{\rho}L}\ ;\ k \in \mathbb{N}^* \tag{43}$$

and the normalized solutions ($\mathcal{L}^2$-norm) are given by

$$B_k = \sqrt{\frac{2}{L}}\sin\left(\frac{k\pi}{L}S\right)\ ;\ k \in \mathbb{N}^* \tag{44}$$

## In plane small vibrations

Now let us focus on (36) and (37). Let us assume that the transverse displacement is given by

$$p = P(S)e^{i\omega t} \tag{45}$$

$$q = Q(S)e^{i\omega t} \tag{46}$$

which can be inserted into (36) and (37) and yields

$$\rho\omega^2 P + EA\left(P' - \mathcal{K}Q\right)' - EA\mathcal{K}\frac{\|\mathbf{r}'\| - 1}{\|\mathbf{r}'\|}(Q' + \mathcal{K}P) = 0 \tag{47}$$

$$\rho\omega^2 Q + EA\left[\frac{\|\mathbf{r}'\| - 1}{\|\mathbf{r}'\|}(Q' + \mathcal{K}P)\right]' + EA\mathcal{K}\left(P' - \mathcal{K}Q\right) = 0 \tag{48}$$

Two types of vibrations may be considered when it comes to planar vibrations. First the anti-symmetric ones that do produce no increment of tension at first order in $\|\mathbf{u}'\|$ and the symmetric ones that produce a uniform increment of tension $\tau$ along the cable at first order in $\|\mathbf{u}'\|$.

**Anti-symmetric modes** Anti-symmetric modes have been historically obtained via assuming that the increment of tension due to vibration is negligible and that the vibration is preponderant in the normal direction. Let us make following assumptions:

- $\frac{\|\mathbf{r}'\|-1}{\|\mathbf{r}'\|}$ can be considered constant with $S$.
- The normal vibration given by $Q$ are preponderant so that (48) is of primary interest and $P$ can be considered second order.
- The variation of the function $\mathcal{K}$ are neglected so we make a first order approximation of it.
- The vibration does not produce any tension increment so that $EA\left(P' - \mathcal{K}Q\right)$, corresponding to the increment of tension, see( 34), is zero.

Then, our assumptions allow one to simplify (48) as follows

$$\rho\omega^2 Q + \alpha^2 Q'' = 0 \quad ; \quad \alpha^2 = EA\,\frac{\|\mathbf{r}'\| - 1}{\|\mathbf{r}'\|} \tag{49}$$

As done in previous paragraph, $Q$ admits as solution

$$Q = q_1 \cos\left(\sqrt{\rho}\frac{\omega}{\alpha}S\right) + q_2 \sin\left(\sqrt{\rho}\frac{\omega}{\alpha}S\right) \tag{50}$$

From the homogeneous boundary conditions, the normal vibration is given by

$$Q_k = q_2 \sin\left(\frac{k\pi}{L}S\right) \ ; \ k \in \mathbb{N}^* \ ; \ k \in \mathbb{N}^* \tag{51}$$

The geometric compatibility condition is given by

$$P' - \mathcal{K}Q = 0 \tag{52}$$

Then

$$P = p_1 - q_1\mathcal{K}\frac{L}{k\pi}\cos\left(\frac{k\pi}{L}S\right) \tag{53}$$

Applying homogeneous boundary condition to $P$ yields

$$P(0) = 0 \leftrightarrow p_1 = q_1\mathcal{K}\frac{L}{k\pi} \tag{54}$$

and then

$$P(L) = 0 \leftrightarrow 0 = q_1\mathcal{K}\frac{L}{k\pi}\left[1 - \cos\left(\frac{k\pi}{L}S\right)\right] \tag{55}$$

Then $k$ must be even to satisfy $P(L) = 0$ creating a vibration which is anti-symmetric with respect to $\frac{L}{2}$ in the normal direction. This is why those vibrations are often denoted as anti-symmetric modes.

As a summary, a mode is given by

$$\omega_k = 2k\frac{\alpha\pi}{\sqrt{\rho}L} \ ; \ k \in \mathbb{N} \tag{56}$$

$$Q_k = \frac{1}{\sqrt{\frac{L}{2} + \frac{3\mathcal{K}^2L^3}{8k^2\pi^2}}}\sin\left(\frac{2k\pi}{L}S\right) \tag{57}$$

$$P_k = \frac{\mathcal{K}L}{k\pi\sqrt{\frac{L}{2} + \frac{3\mathcal{K}^2L^3}{8k^2\pi^2}}}\sin\left(\frac{k\pi}{L}S\right)^2 \tag{58}$$

It is worth noting that those modes are not orthogonal in the sense of the following inner-product

$$(P_i, Q_i) \times (P_j, Q_j) \longrightarrow \int_0^L P_iP_j + Q_iQ_j \mathrm{d}S \tag{59}$$

**Symmetric modes** Let us make following assumptions:

- $\frac{\|\mathbf{r}'\|-1}{\|\mathbf{r}'\|}$ can be considered constant with $S$.
- The normal vibration given by $Q$ are preponderant so that (48) is of primary interest and $P$ can be considered

second order.

- The variation of the function $\mathcal{K}$ are neglected so we make a first order approximation of it.
- The vibration produces a tension increment which is a function of time alone. Then the function $EA\,(P' - \mathcal{K}Q)$, corresponding to the increment of tension, can be consider to be constant with space and its value is given by $\tau$.

These assumptions lead to a simplified version of (48) which is

$$\rho\omega^2 Q + \alpha^2 Q'' = -\mathcal{K}\tau \quad ; \quad \alpha^2 = EA\,\frac{\|\mathbf{r}'\| - 1}{\|\mathbf{r}'\|} \tag{60}$$

The latter implies that

$$Q = q_1 \cos\left(\sqrt{\rho}\frac{\omega}{\alpha}S\right) + q_2 \sin\left(\sqrt{\rho}\frac{\omega}{\alpha}S\right) - \frac{\mathcal{K}}{\rho\omega^2}\tau \tag{61}$$

From compatibility condition, we have that

$$P = p_1 + q_1\frac{\mathcal{K}\alpha}{\omega\sqrt{\rho}}\sin\left(\sqrt{\rho}\frac{\omega}{\alpha}S\right) - q_2\frac{\mathcal{K}\alpha}{\omega\sqrt{\rho}}\cos\left(\sqrt{\rho}\frac{\omega}{\alpha}S\right) + \left(\frac{1}{EA} - \frac{\mathcal{K}^2}{\rho\omega^2}\right)\tau S \tag{62}$$

Homogeneous boundary conditions lead to the following determinental equation

$$\begin{bmatrix} 1 & 0 & 0 & -\frac{\mathcal{K}}{\omega^2\rho} \\ \cos\left(\sqrt{\rho}\frac{\omega}{\alpha}L\right) & \sin\left(\sqrt{\rho}\frac{\omega}{\alpha}L\right) & 0 & -\frac{\mathcal{K}}{\omega^2\rho} \\ 0 & -\frac{\alpha\mathcal{K}}{\omega\sqrt{\rho}} & 1 & 0 \\ \frac{\alpha\mathcal{K}}{\omega\sqrt{\rho}}\sin\left(\sqrt{\rho}\frac{\omega}{\alpha}L\right) & -\frac{\alpha\mathcal{K}}{\omega\sqrt{\rho}}\cos\left(\sqrt{\rho}\frac{\omega}{\alpha}L\right) & 1 & L\left(\frac{1}{EA} - \frac{\mathcal{K}^2}{\rho\omega^2}\right) \end{bmatrix} \begin{bmatrix} q_1 \\ q_2 \\ p_1 \\ \tau \end{bmatrix} = \begin{bmatrix} 0 \\ 0 \\ 0 \\ 0 \end{bmatrix} \tag{63}$$

which can be recast into the following transcendental equation in $\omega$

$$\mathcal{F}(\omega) = \tan\left(\frac{\omega\sqrt{\rho}L}{2\alpha}\right) - \frac{\omega\sqrt{\rho}L}{2\alpha}\left(\mathcal{K}^2 EA - \omega^2\rho\right) = 0 \tag{64}$$

$$\iff \tan\left(\frac{\omega\sqrt{\rho}}{2\alpha}L\right) = \frac{\mathcal{K}^2 EA\sqrt{\rho}L}{2\alpha}\omega - \frac{\sqrt{\rho}^3 L}{2\alpha}\,\omega^3 \tag{65}$$

where the cases $\omega = 0$ and $\omega = k\frac{\alpha\pi}{\sqrt{\rho}L}$ are discarded.

From a practical point of view, only the very first solutions will be of interest since the cubic function rapidly intersects the infinite branch of the $\tan$ function (i.e. we reach the case $\omega = k\frac{\alpha\pi}{\sqrt{\rho}L}$ ).

**A remark on equation (65)** Solving this equation reveals to be numerically challenging, especially with descent methods (e.g. Newton's method). A way to tackle it, is to perform dichotomy on sub-intervals where $\tan$

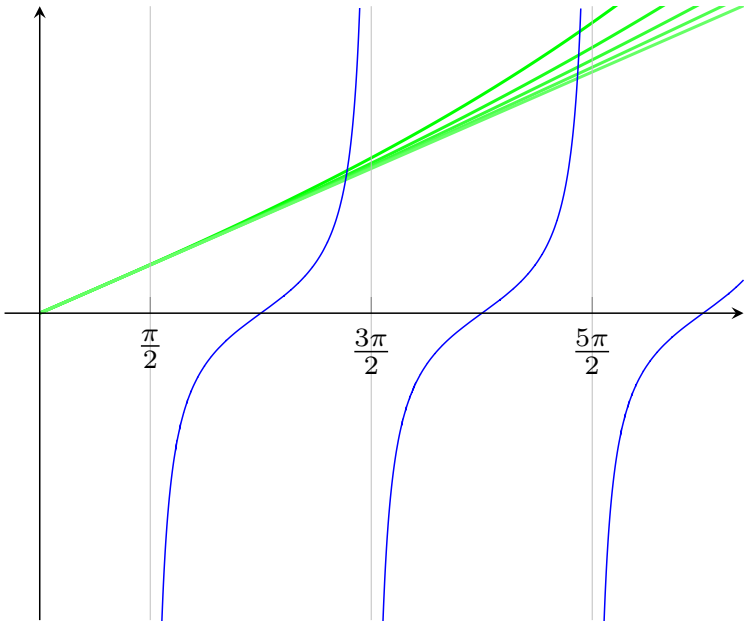


Figure 2: Transcendental equation (65) for various values of system parameters - $\tan$ plot (solid line —) - cubic plot (solid line —)

will change of sign. The graphs of the two functions are depicted into Figure 2. It can be seen that for $X$ close to $\frac{2k+1}{2}\pi$, $\tan X$ is greater than the cubic function of $X$ so that dichotomy can be applied in a vicinity of it. The algorithm applied to (65) is given in Algorithm 1.

# Nonlinear dynamics of a forced hanging cable

In this section the equations for the nonlinear dynamics of a hanged cable are presented. It is often assumed that the main dynamic content of a cable is contained into its vibrations along the first modes. Our choice is to keep the influence of the longitudinal motions in the projection and to use numerical based methods that can be applied to general cases with an arbitrary number of dof.

## Ritz-Galerkin procedure

From this statement, one can choose to project the nonlinear dynamics on a family of chosen modes computed in Section . The modes can also be extracted directly from (37 - 38) via finite differences methods [11]. The latter is more suitable to retain the influence of system curvature and tension on the modes and frequencies. The methodology has already been endowed by the authors in [9].

Then the displacement is given by

$$\mathbf{u}(S,t) = \sum_{k=1}^{N} \Phi_k(S)\varphi_k(t) \tag{66}$$

**Needed:** ;
*Number of expected solutions:* $N$ ;
*Coefficient:* $c$ ;
**Initialize:** ;
$X \leftarrow (0, ..., \frac{2N+3}{2}\pi)$ (small mesh) ;
$X^+ \leftarrow X[2;;\text{end}]$ ;
$X^- \leftarrow X[1;;\text{end}-1]$ ;
$X^* \leftarrow X^+ \times X^-$ ;
$\omega \leftarrow X^+[k \text{ such that } X^*_k <= 0]$ ;
$\bar{\omega} \leftarrow X^-[k \text{ such that } X^*_k <= 0]$ ;
Limit $\omega$ and $\bar{\omega}$ to their first $N^{\text{th}}$ components ;
**for** $1 \leq i \leq 50$ **do**
    $f^+ \leftarrow \mathcal{F}(\frac{\omega+\bar{\omega}}{2})$ (size $N$);
    $f^- \leftarrow \mathcal{F}(\bar{\omega})$ (size $N$);
    **if** $f^+_k \times f^-_k <= 0$ **then**
        $\omega_k \leftarrow \frac{\omega+\bar{\omega}}{2}$
    **end**
    **if** $f^+_k \times f^-_k > 0$ **then**
        $\bar{\omega}_k \leftarrow \frac{\omega+\bar{\omega}}{2}$
    **end**
**end**
**Return** $\omega$

**Algorithm 1:** Dichotomy approach for numerical treatment of (65)

where $\Phi_k$ is a cable mode. Note that, projections can be performed on arbitrary modes.

The actual tension is obtained as a Taylor expansion up to third order in $\|\mathbf{u}'\|$:

$$\begin{aligned} EA\left(\|\mathbf{R}'\|-1\right)\frac{\mathbf{R}'}{\|\mathbf{R}'\|} =& EA(\|\mathbf{r}'\|-1)\mathbf{e} \\ &+EA\frac{\|\mathbf{r}'\|-1}{\|\mathbf{r}'\|}\mathbf{u}'+\frac{EA}{\|\mathbf{r}'\|}(\mathbf{e}\cdot\mathbf{u}')\mathbf{e} \\ &+\frac{EA}{2\|\mathbf{r}'\|^2}\left(\left[\mathbf{u}'\cdot\mathbf{u}'-3(\mathbf{e}\cdot\mathbf{u}')^2\right]\mathbf{e}+2\left[\mathbf{e}\cdot\mathbf{u}'\right]\mathbf{u}'\right) \\ &+\frac{EA}{2\|\mathbf{r}'\|^3}\begin{pmatrix}\left[5(\mathbf{e}\cdot\mathbf{u}')^3-3(\mathbf{e}\cdot\mathbf{u}')(\mathbf{u}'\cdot\mathbf{u}')\right]\mathbf{e} \\ +\left[\mathbf{u}'\cdot\mathbf{u}'-3(\mathbf{e}\cdot\mathbf{u}')^2\right]\mathbf{u}'\end{pmatrix} \end{aligned} \tag{67}$$

Equation (67) can be seen seen as the superposition of static elastic forces, $f_e(\mathbf{r})$, and incremental elastic forces due to the vibration, $\Delta f_e(\mathbf{r},\mathbf{u})$, i.e.

$$EA\left(\|\mathbf{R}'\|-1\right)\frac{\mathbf{R}'}{\|\mathbf{R}'\|} = f_e(\mathbf{r}) + \Delta f_e(\mathbf{r},\mathbf{u}) \tag{68}$$

The incremental elastic forces, $\Delta f_e(\mathbf{r},\mathbf{u})$, are recasted in the Frenet basis as follows

$$\begin{aligned}\Delta f_e(\mathbf{r},\mathbf{u}) =& EA\begin{bmatrix} p'-\mathcal{K}q \\ 0 \\ 0 \end{bmatrix} + EA\frac{\|\mathbf{r}'\|-1}{\|\mathbf{r}'\|}\begin{bmatrix} 0 \\ q'+\mathcal{K}p \\ b \end{bmatrix} \\ &+\frac{EA}{2\|\mathbf{r}'\|^2}\begin{bmatrix} (q'+\mathcal{K}p)^2+b^2 \\ 2\left(p'-\mathcal{K}q\right)\left(q'+\mathcal{K}p\right) \\ 2\left(p'-\mathcal{K}q\right)b \end{bmatrix} \\ &-\frac{EA}{2\|\mathbf{r}'\|^3}\begin{bmatrix} 2\left(p'-\mathcal{K}q\right)\left[(q'+\mathcal{K}p)^2+b^2\right] \\ \left[2\left(p'-\mathcal{K}q\right)^2-(q'+\mathcal{K}p)^2-b^2\right](q'+\mathcal{K}p) \\ \left[2\left(p'-\mathcal{K}q\right)^2-(q'+\mathcal{K}p)^2-b^2\right]b \end{bmatrix}\end{aligned} \tag{69}$$

The full nonlinear dynamics yields

$$\rho\ddot{\mathbf{R}}+2\mu\dot{\mathbf{R}} = \left[f_e(\mathbf{r})+\Delta f_e(\mathbf{r},\mathbf{u})\right]'+\mathbf{b}+f(S,t) \tag{70}$$

Simplifying (70) thanks to (11) yields

$$\rho\ddot{\mathbf{u}}+2\mu\dot{\mathbf{u}}-\left[\Delta f_e(\mathbf{r},\mathbf{u})\right]' = f(S,t) \tag{71}$$

A Ritz-Galerkin procedure is performed with respect to the inner-product given in (59). The case presented here is general and accounts for any external forcing considered. It should be noted that even the longitudinal component of the motion is kept in the following developments. $N$ equations are obtained as follows

$$\int_0^L(\rho\ddot{\mathbf{u}}+2\mu\dot{\mathbf{u}})\cdot\Phi_j\mathrm{d}S+\int_0^L\Delta f_e(\mathbf{r},\mathbf{u})\cdot\Phi_j'\mathrm{d}S = \int_0^L f(S,t)\cdot\Phi_j\mathrm{d}S \quad , \quad 1\leqslant j\leqslant N \tag{72}$$

where the differentiation of vectors with regards to $S$ is done via (30).

In the case presented here, the mass matrix and stiffness matrix are non-diagonal which is the cost of the generality of the approach. The latter is due to the loss of symmetry in the Ritz-Galerkin procedure. The obtained system reads

$$\mathbf{M}_{jk}\ddot{\varphi}_k+\mathbf{C}_{jk}\dot{\varphi}_k+\mathbf{K}_{jk}\varphi_k+\mathcal{Q}_{jkl}\varphi_k\varphi_l+\mathcal{C}_{jklm}\varphi_k\varphi_l\varphi_m = \mathbf{f}_j \quad , \quad 1\leqslant j\leqslant N \tag{73}$$

where Einstein convention has been used. The formal expression of each tensor is given in appendix 22. To lighten numerical computations, we premultiplied by the mass matrix inverse and used a rescaled time allows to obtain the

following system

$$\ddot{\varphi}_j + \xi_j \dot{\varphi}_j + \mathbf{K}_{jk}\varphi_k + \mathcal{Q}_{jkl}\varphi_k\varphi_l + \mathcal{C}_{jklm}\varphi_k\varphi_l\varphi_m = \mathbf{f}_j \quad , \quad 1 \leqslant j \leqslant N$$
$$t = \frac{\tau}{\omega_0} \tag{74}$$

for conciseness we did not change the notation for $\mathbf{K}$, $\mathcal{Q}$, $\mathcal{C}$ and $\mathbf{f}$. The obtained ROM is general and accounts for longitudinal, normal and transversal displacements. The rich coupling between modes is given by both the non-diagonal mass matrix and the quadratic/cubic nonlinearities.

## Tracking frequency response with arc-length continuation technique

The set of equations given by (74) can be numerically treated with the arc-length method [10, 51]. The key idea is to follow the response curve assuming that the latter is smooth and that the system response is periodic. The system is harmonically forced with an arbitrary frequency $\Omega$, in another words we set

$$f(S,t) = F(S)\sin(\Omega t) \tag{75}$$

To obtain the system response, we track fixed points of the monodromy matrix [13] and the stability of the response is estimated via evaluating the eigenvalues of the same matrix at a converged state. Indeed, considering an initial condition $\varphi^*$ the problem reads

$$\mathcal{M}(\varphi^*, \Omega)\ \varphi^*(0) = \varphi^*\left(\frac{2\pi}{\Omega}\right) \tag{76}$$

When a couple $(\varphi^*, \Omega)$ satisfies (76), the stability of this periodic orbit is determined as follows:

- Stable if all eigenvalues is contained in the unit circle
- Unstable if at least one eigenvalue is out of the unit circle

An example have been done for the set of parameters given in Table 1 and the corresponding response curves are given in Figure 3. The plots are done with regard to the normalized frequency and for a 5 dofs projection. The odd dofs correspond here to the transverse modal coordinates whereas the even dofs correspond to the planar modal coordinates. The response is sophisticated and multi-valued, therefore the design of cable requires an in-depth analysis of their frequency responses. This simple example also depicts potential large displacements close to resonance. The components of the various tensors in (74) are given in appendix 22. However, we must recall that amplitudes caught in the ROM should be analyzed in the scope of the physical amplitude at stake via usage of (66).

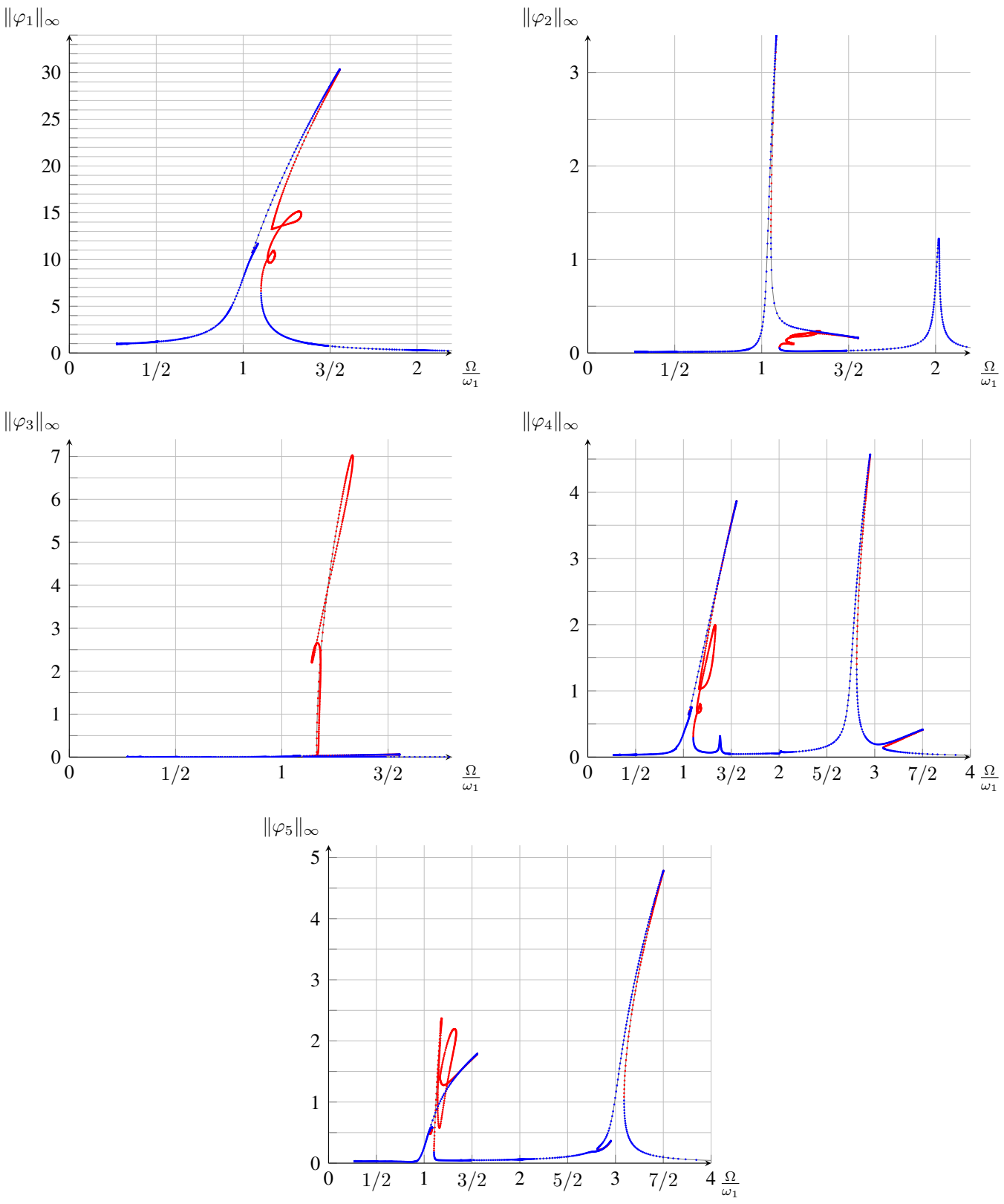


Figure 3: Frequency response curves obtained with arc-length continuation technique for a 5 dof system (dotted line ·····) Stable solutions ; (dotted line ·····) Unstable solutions

Table 1: Parameters used for the arc-length continuation example (Physical value of a chair-lift span)

| Attributes | Values |
|---|---|
| $EA$ (N) | $4 \times 10^8$ |
| $T_0$ (N) | 80000 |
| $\rho$ (kg.m$^{-1}$) | 6 |
| $d$ (m) | 250 |
| $h$ (m) | 10 |
| $\mu$ | 0.08 |
| $F(S)$ (N) | $0.8\,(\mathbf{e}+\mathbf{n}+\mathbf{z})$ |

# A comparison with Finite Element Method (FEM)

The usage of ROM is mainly drove by its computational efficiency and the possibility of studying analytically small-dof systems. However, very few comparisons between results of finite element and those of ROM are available.

FEM has been already developed to ensure tension-state during computations [8], the latter has been proven reliable and to converge towards what we can called a reference solution. This claim is briefly illustrated by Figure 4 where the trajectory at mid-span is obtained via FEM where the time-step is decreased progressively. Table 2 provides with the numerical error made by considering wider time-steps, taking a converged solution as a reference. This error is taken as the relative error made on displacements at multiple of the period of solicitation. In another words, the error on the coordinates of the midspan at all $k \times T$ with k = 1,...,7 is given. Those examples are meant to further illustrates the convergence properties of the FEM used in this paper and presented in [8]. FEM computations and the approach presented before have some intrinsic differences among which:

- In FEM, the nonlinear dynamics are integrated with the self-weight effects retained and the assumption of a small displacement is not made
- In the ROM, amplitudes correspond to modal coordinates so that the displacement profile needs to be built back
- In the ROM, the vibration around the rest position is an elastic vibration, therefore inextensible/inelastic motions could be roughly approximated.

The goal of this subsection is to compare the predictions made by both methods and have a claim on the validity of the reduce-order model. This comparison is based on the following steps:

- With the same set of parameters, compute the dynamics of the cable via the ROM and the FEM
- Build back the cable profile from the ROM according to (66)

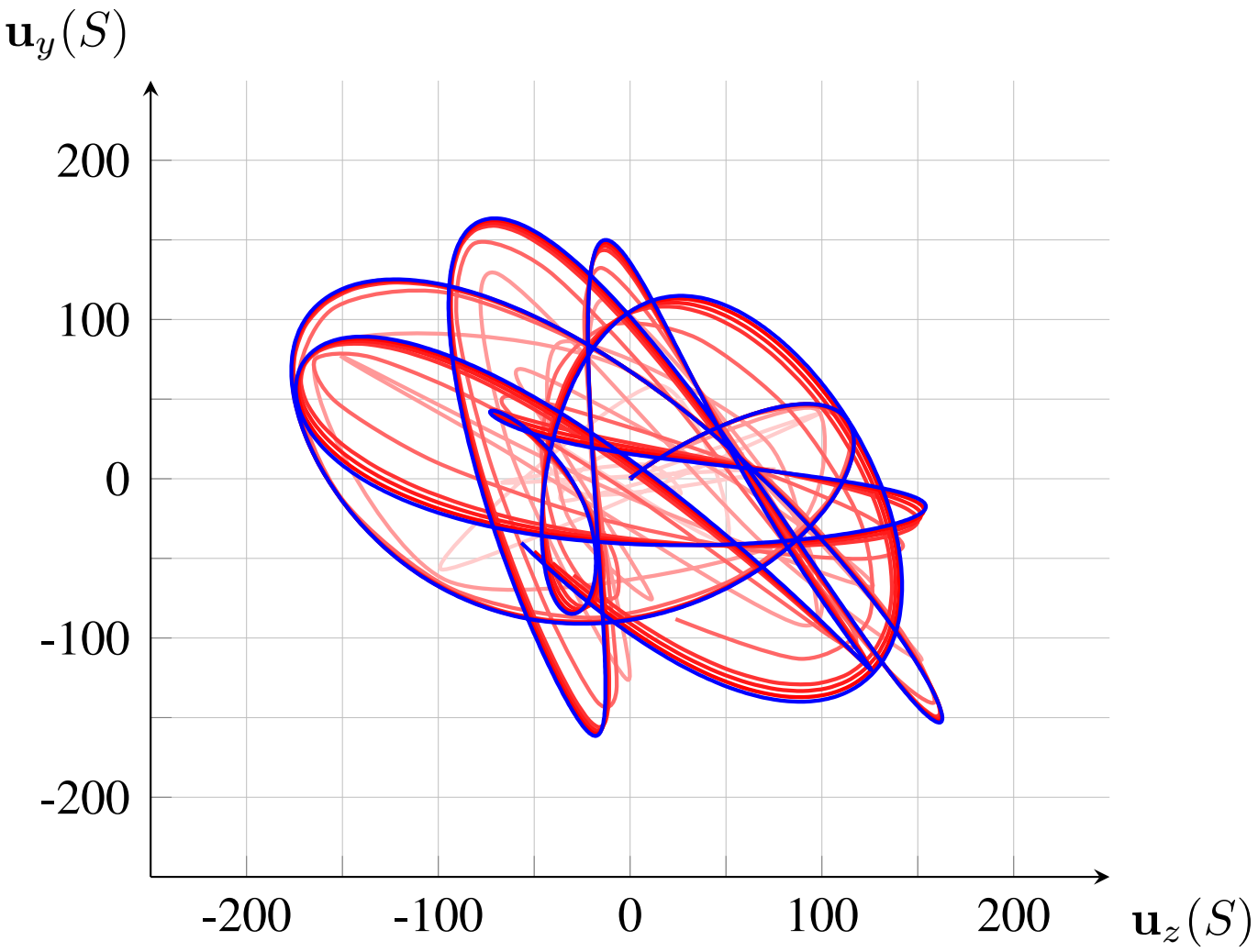


Figure 4: Cable with parameters given in Table 3 integrated with varying time-steps, spanning from $h = 0.0011$s to $h = 0.06$s (solid line —) and with $h = 0.0003$s (solid line —)

- Compare the transient trajectories at given point of the span in the physical domain
- Compare the evaluation of system amplitude at first $(\mathbf{u}_{\text{fqs}})$ and last quarter span $(\mathbf{u}_{\text{lqs}})$ and at mid-span $(\mathbf{u}_{\text{ms}})$ in the physical domain with different forcing amplitude. The latter will be performed via continuation technique on the ROM while the NFEM dynamics will be integrated until a stationary point is reached.

### Comparisons of Transient Dynamics

The transient dynamics are of deep interest for engineering applications due to potential high displacements. The ability of reduced-order-model to track such responses could avoid costful computations via refined mesh in NFEM. Different scenarios are investigated here. System amplitudes are checked close and far from resonances and with different configurations (highly and moderately tensed). The set of parameters depicted in Table 3 are used for the results depicted on Figures 5 - 8. The idea between those two different scenarios is that one case corresponds to a

Table 2: Numerical error obtained from integrating the cable dynamics given in Table 3 with the FEM with varying time-steps

| Time step (s) | Error at : | $t = T$ | $t = 2T$ | $t = 3T$ | $t = 4T$ | $t = 5T$ | $t = 6T$ |
|---|---|---|---|---|---|---|---|
| 0.01197 | | 0.7860 | 0.9053 | 0.8269 | 0.8809 | 1.0012 | 0.7913 |
| 0.00399 | | 0.0343 | 0.0825 | 0.332 | 0.228 | 0.167 | 0.3229 |
| 0.00249 | | 0.0112 | 0.0263 | 0.1136 | 0.0799 | 0.0528 | 0.1219 |
| 0.00120 | | 0.0067 | 0.0157 | 0.0686 | 0.0484 | 0.0313 | 0.0749 |
| 0.00030 | | 0.0027 | 0.0064 | 0.0284 | 0.0202 | 0.0128 | 0.0315 |

linear regime in the sense that nonlinearities cannot have significant impact on the response whereas in the other case, the geometry and forcing amplitude lead to a response where the nonlinearities are essential to describe the system response.

For the quasi-linear regime (taut cable with small forcing amplitude), we see a qualitatively good agreement between both approaches as illustrated by Figure 5. The overall motion of the cable is described similarly so that the maximum amplitudes of vibrations will be the same. However, the ROM is way faster due to its compactness. The envelop of the cable motion is also well approximated as shown in Figure 6. Indeed, both FEM and ROM provide with same displacement amplitude in this case although it is transient dynamics.

When it comes to the nonlinear case, the qualitative agreement holds. However, discrepancies in the longitudinal direction arises. The small differences can be explained by the difference in the treatment of the geometrical nonlinearity since it is linearized up to third order in the ROM. Some specific scenarios, especially resonant cases, produce quantitative differences between the FEM prediction and the ROM prediction. This points to the fact that ROM may not always be the good tool to describe the cable dynamics.

Computational speed is the key parameter to choose one of the approaches, although FEM may be more flexible when it comes to compute the response of more complicated systems (e.g. cable networks, hybrid boundary conditions, beam-cable structures, ...). The main advantage of the ROM is the possibility of pseudo-analytical solutions but it relies on very practical knowledge of cable nonlinear dynamics and behaviors [5, 54] which is not the topic of this work. Moreover, the more DOFs are of interest, the less intuitive are the analytical derivations. In this case, FEM are reliable tool to investigate nonlinear dynamics of a unknown cable system and determine the applicability of the ROM, see for example Figure 7.

Table 3: Parameters used for the comparisons between transient dynamics caught via FEM and ROM

| Attributes | Values (Linear case) | Values (Nonlinear case) |
|---|---|---|
| $EA$ (MN) | 40 | 10 |
| $T_0$ (MN) | 1.116 | 0.8 |
| $\rho$ (kg.m$^{-1}$) | 5.56 | 5.56 |
| $d$ (m) | 300 | 300 |
| $h$ (m) | 10 | 15 |
| $\mu$ (SI) | 0.08 | 0.08 |
| $F(S)$ (N) | $0.0001 \begin{bmatrix} 1 \\ 1 \\ 1 \end{bmatrix}_{(\mathbf{x},\mathbf{y},\mathbf{z})}$ | $0.8 \begin{bmatrix} 1 \\ 1 \\ 1 \end{bmatrix}_{(\mathbf{x},\mathbf{y},\mathbf{z})}$ |
| $\Omega$ (rad/s) | 1.5 | 2.1 |

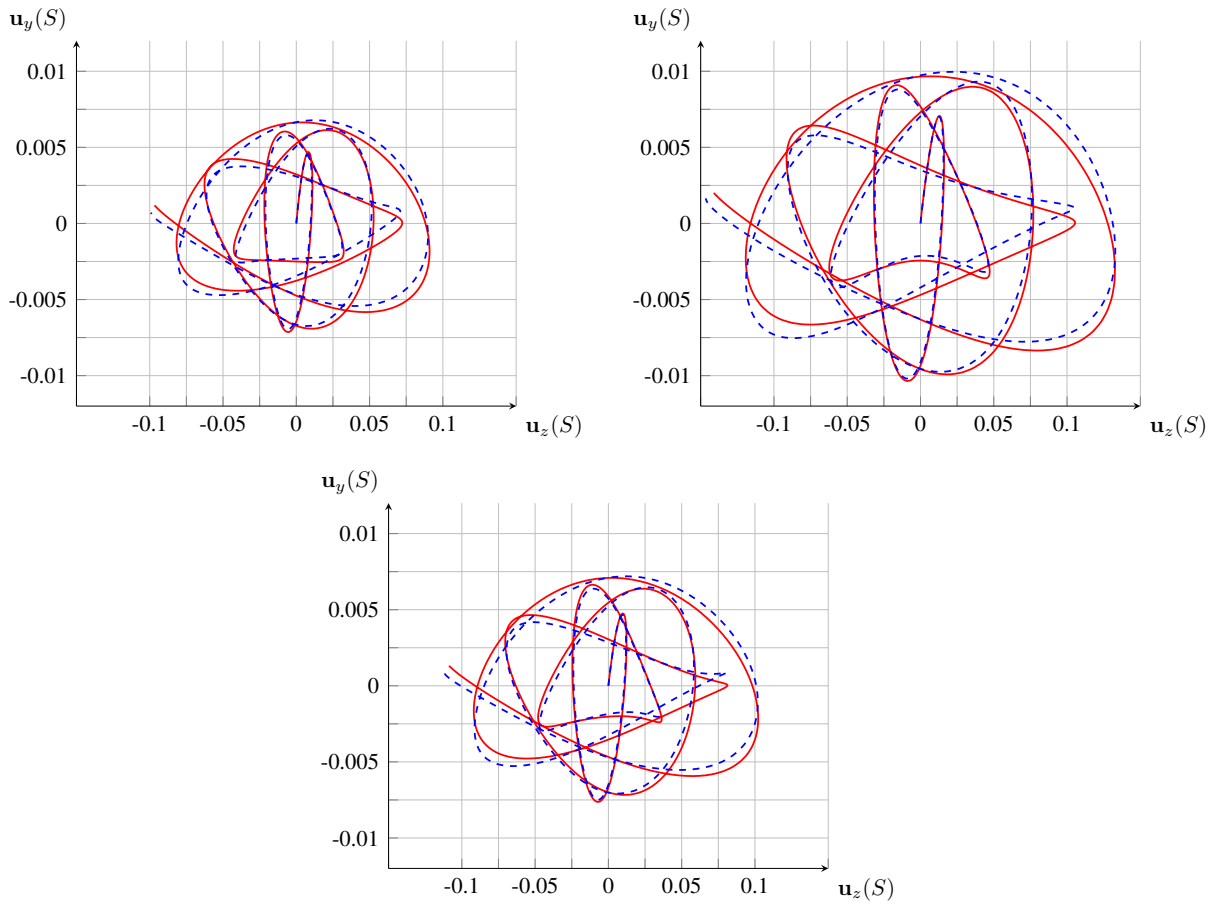


Figure 5: Vertical displacement versus transverse displacement (mm) for $S = \frac{L}{4}$, $S = \frac{L}{2}$ and $S = \frac{3L}{4}$ obtained via FEM (solid line —) and via ROM (dashed line - - -) for a transient dynamics in a quasi-linear regime - Parameters are given in Table 3

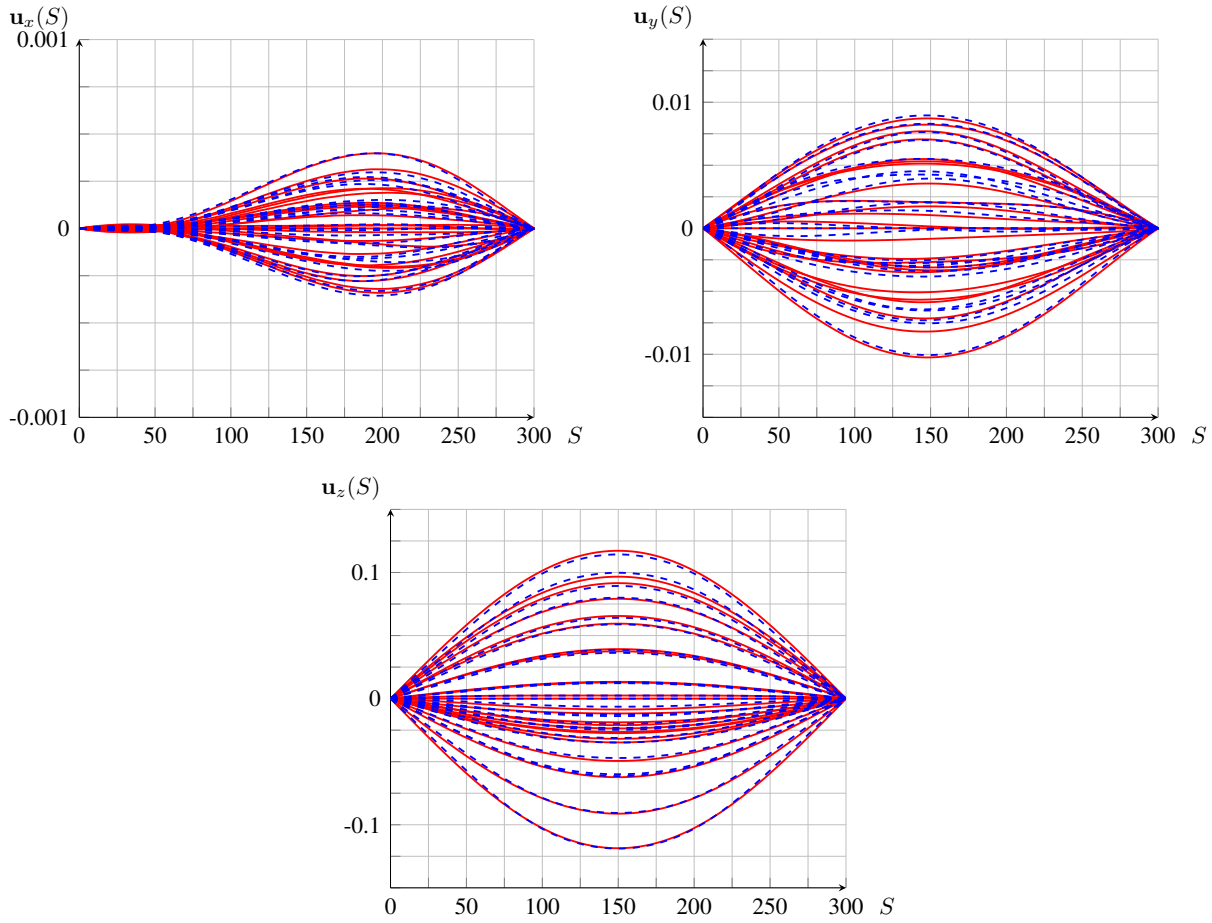


Figure 6: Displacement (mm) versus curvilinear abscissa (m) for the $\mathbf{x}$ direction, $\mathbf{y}$ direction and $\mathbf{z}$ direction obtained via FEM (solid line —) and via ROM (dashed line - - -) for a transient dynamics in a quasi-linear regime at the same time instants - Parameters are given in Table 3

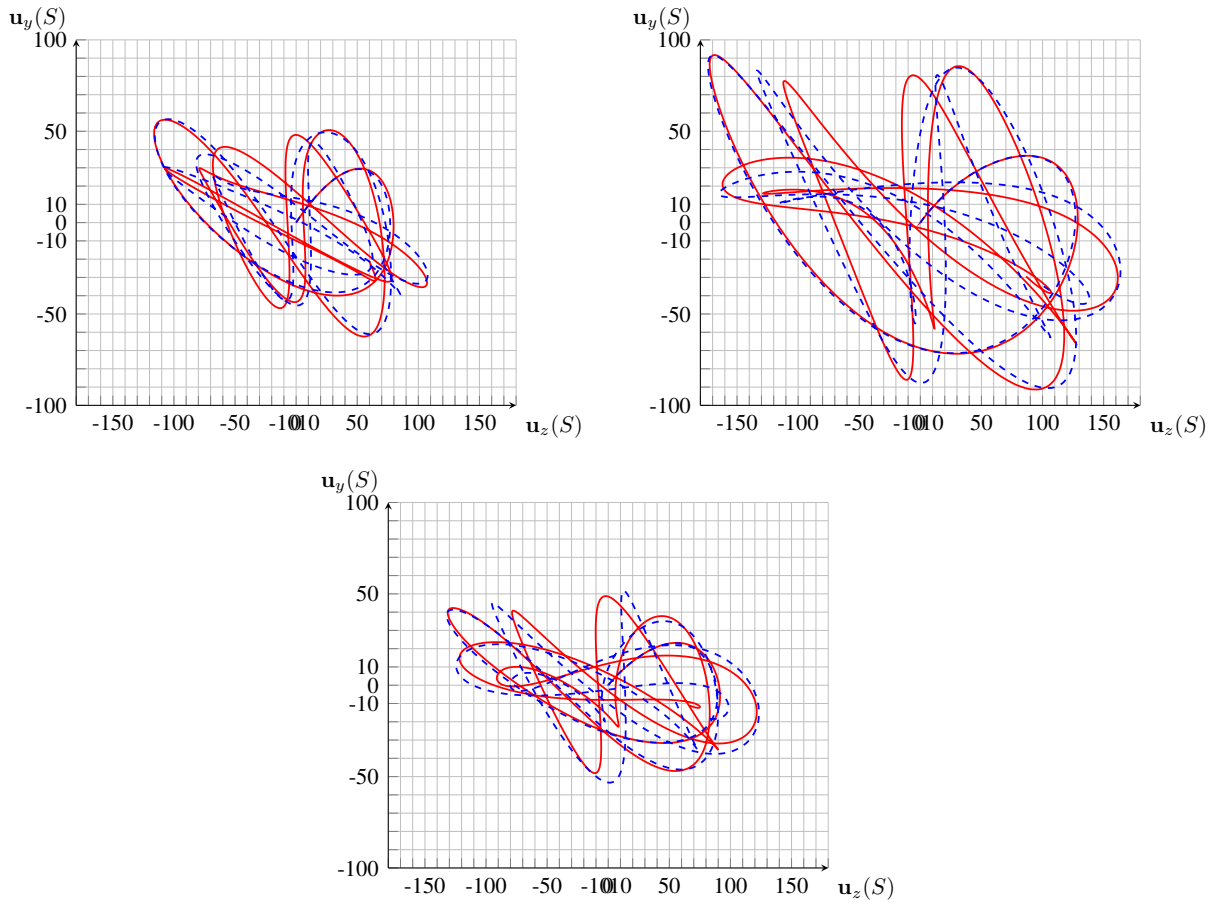


Figure 7: Vertical displacement versus transverse displacement (mm) for $S = \frac{L}{4}$, $S = \frac{L}{2}$ and $S = \frac{3L}{4}$, span obtained via FEM (solid line —) and via ROM (dashed line - - -) for a transient dynamics in a nonlinear regime - Parameters are given in Table 3

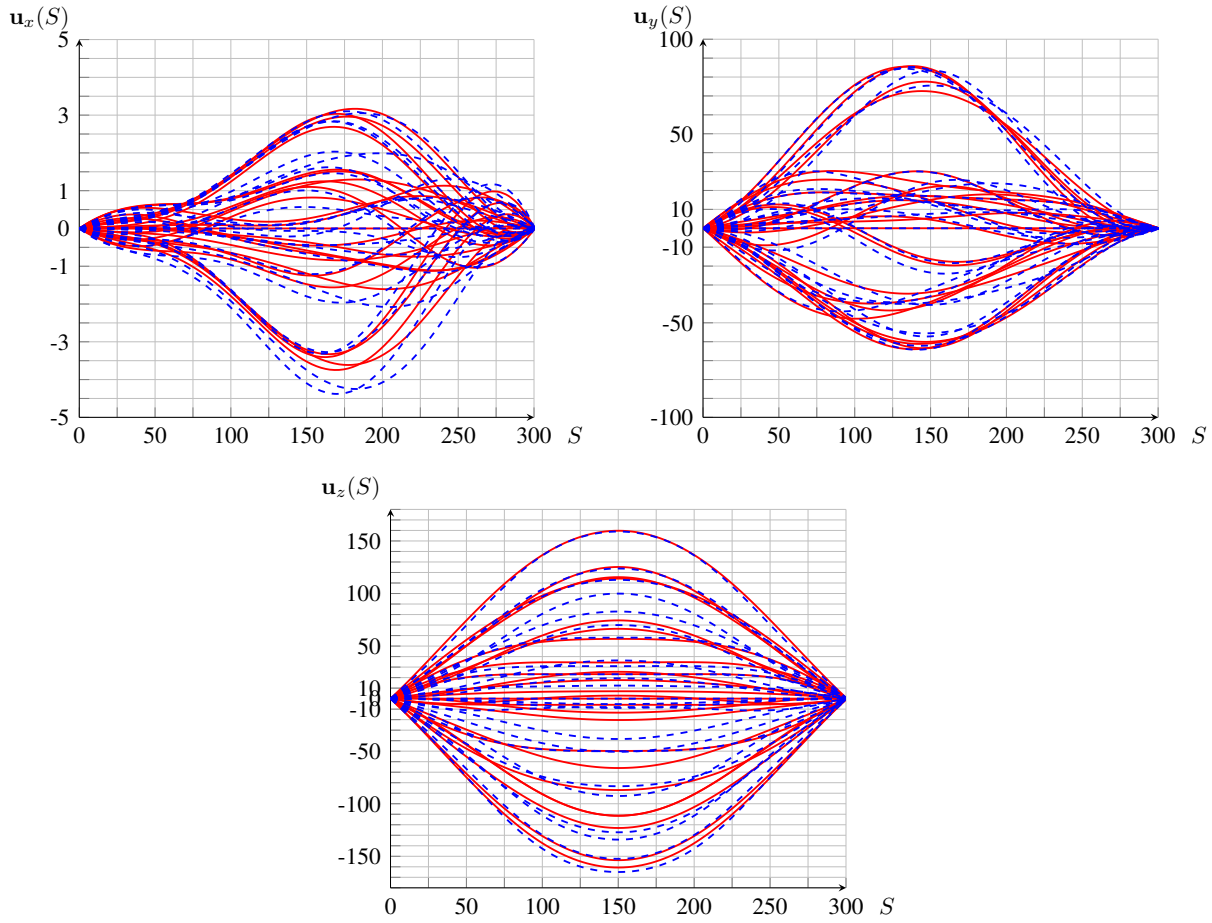


Figure 8: Displacement (mm) versus curvilinear abscissa (m) for the $\mathbf{x}$ direction, $\mathbf{y}$ direction and $\mathbf{z}$ direction obtained via FEM (solid line ——) and via ROM (dashed line - - -) for a transient dynamics in a nonlinear regime - Parameters are given in Table 3

Table 4: Parameters used for the comparisons between asymptotic dynamics caught via FEM and ROM

| Attributes | Values (Linear case) | Values (Nonlinear case) |
|---|---|---|
| $EA$ (MN) | 40 | 10 |
| $T_0$ (MN) | 1.116 | 0.8 |
| $\rho$ (kg.m$^{-1}$) | 5.56 | 5.56 |
| $d$ (m) | 300 | 300 |
| $h$ (m) | 15 | 15 |
| $\mu$ (SI) | 0.2 | 0.2 |
| $F(S)$ (N) | $0.0001\,(\mathbf{x}+\mathbf{y}+\mathbf{z})$ | $0.8\,(\mathbf{x}+\mathbf{y}+\mathbf{z})$ |
| $\Omega$ (rad/s) | 1.5 | 2.1 |

## Comparisons of Asymptotic Dynamics

Dynamic simulations are costful especially with NFEM. The ROM is therefore a valuable tool to describe rich dynamic behavior since of the light computational effort needed. Due to the system dimension, continuation techniques are not a good fit for tracing the NFEM asymptotic dynamic responses. This is why ROM are better suited for arc-length continuation. A comparison between asymptotic responses of the NFEM dynamics and the ROM response computed via continuation method is proposed here. The goal of this comparison is to assess for the reliability of designs relying of ROM and also for the NFEM ability to trace nonlinear behaviors.
The parameters, used for the computations are given in Table 4. Every computations have been performed with a time step such that the smallest period at stake is divided into 2000 intervals.

From Figures 9 - 10, we can see that the linear regimes are well reconstituted by both approaches. The amplitudes at first-quarter span, mid-span and last-quarter span are given respectively by $\mathbf{u}_{\text{fqs}}$ , $\mathbf{u}_{\text{ms}}$ and $\mathbf{u}_{\text{lqs}}$. In this case, the assumptions made for obtaining the ROM (see Section ) do not have any impact on the obtained amplitudes. However the highly-nonlinear regime responses obtained from FEM and the ROM are different. For low frequencies, the two predictions of amplitude are still qualitatively in agreement, but with higher frequencies come more discrepancies. It appears that coupling between modes are not always traced by the ROM and that the latter tends to overestimate the amplitude of displacement. Additional modes may be added in the continuation to catch further details about the nonlinear dynamics however some discrepancy subsist between both approaches in the nonlinear case. Even though the modes obtained via FEM and ROM are the same, it is difficult to keep a good match between dynamic responses when the cable is slacker, inclined and subjected to moderate loads. To accommodate this issue, the usage of ROM

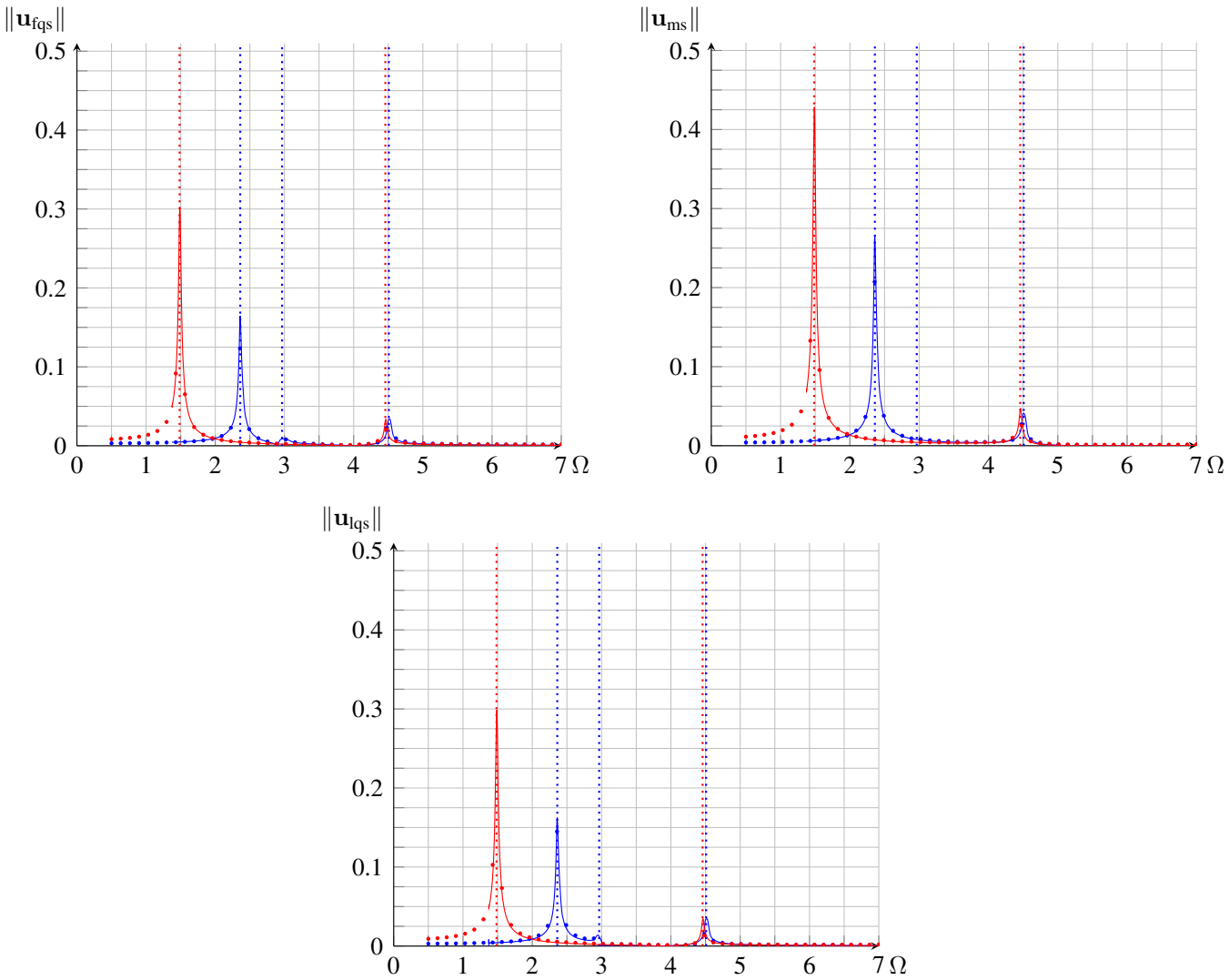


Figure 9: Displacement (mm) versus frequency of forcing (rad/s) for the y direction and z direction obtained via FEM (dots •) and (dots •) and via arc-length continuation endowed in the ROM (solid line —) and (solid line —) in a linear regime - From left to right first quarter span , midspan and last quarter span - Undamped frequencies are plotted vertically - Parameters are given in Table 4

should be always supported by another tool, especially in the latter case.

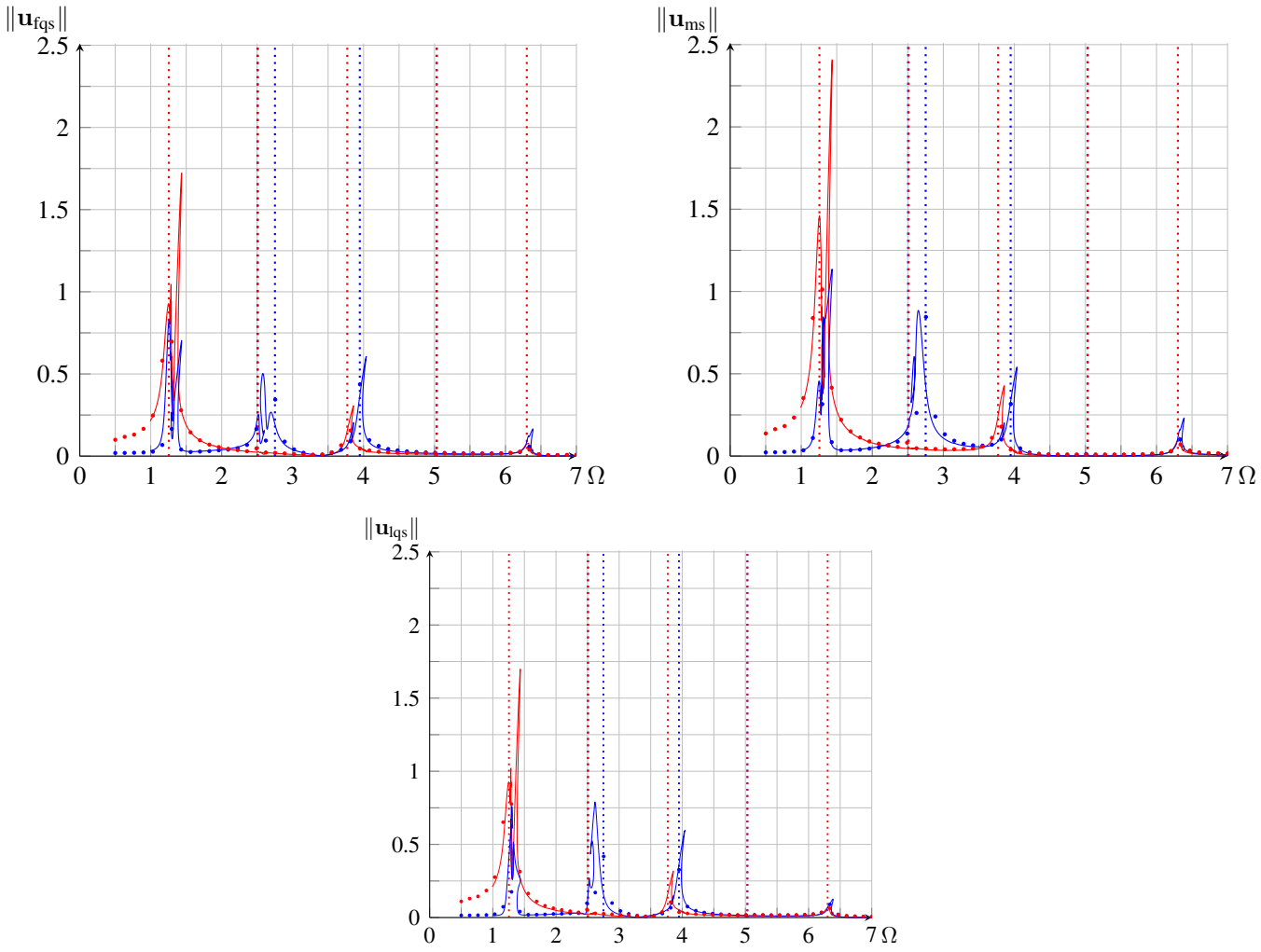


Figure 10: Displacement (m) versus frequency of forcing (rad/s) for the $\mathbf{y}$ direction and $\mathbf{z}$ direction obtained via FEM (dots •) and (dots •) and via arc-length continuation endowed in the ROM (solid line —) and (solid line —) in a nonlinear regime - From left to right first quarter span , midspan and last quarter span - Undamped frequencies are plotted vertically - Parameters are given in Table 4

# Conclusion

The current work entails the governing equations for an elastic cable. The case of the statics is studied analytically. From the static configuration, essential feature of the theory of cable vibration are derived in the Frenet basis which allows to capture the frequencies and modes.

A Ritz-Galerkin projection technique is used to obtain a reduced-order-model which can trace the nonlinear dynamics of a cable subjected to an arbitrary load. The longitudinal, normal and transversal motions are faithfully described by the approach. An example of frequency curve is provided which is obtained via arc-length continuation technique.

The presented methodology is general and applicable for an arbitrary number of degrees of freedom systems without neglecting the longitudinal displacement.

The reliability of the reduced-order-model for transient dynamics and for asymptotic responses have been assessed and discussed via comparisons with nonlinear finite element models. It appears that both approaches are complementary. Indeed, the relevance of reduced-order-model in the case of large amplitudes should be checked via suitable numerical approaches to ensure that predictions of the system responses and its design takes into account the physics at stake.

# Data availability

The authors confirm that the data supporting the findings of this study are available within the article or its supplementary materials.

# Acknowledgments

The authors gratefully thank the 'Ministère de la Transition Écologique' for its financial support.

# Formal values for the tensors

Let us consider here that $\Phi$ refers to a mode and its subscript refers to its index. The latter can be decomposed in the Frenet basis as follows

$$\Phi_j = \begin{bmatrix} P_j \\ Q_j \\ B_j \end{bmatrix} \tag{77}$$

$$\mathbf{M}_{jk} = \rho \int_0^L \Phi_j \cdot \Phi_k \mathrm{d}S \tag{78}$$

$$\mathbf{C}_{jk} = 2\mu \int_0^L \Phi_j \cdot \Phi_k \mathrm{d}S \tag{79}$$

As we work in the Frenet basis, the derivative of a given mode reads

$$\Phi'_j = \begin{bmatrix} P'_j - \mathcal{K} Q_j \\ Q'_j + \mathcal{K} P_j \\ B'_j \end{bmatrix} \tag{80}$$

The latter allows to take into account the curvature into the first, second and third order expansion of the elastic forces in the nonlinear equations of the motion (73) .

$$\mathbf{K}_{jk} = EA \int_0^L \left( \begin{bmatrix} P'_k - \mathcal{K} Q_k \\ 0 \\ 0 \end{bmatrix} + \frac{\|\mathbf{r}'\| - 1}{\|\mathbf{r}'\|} \begin{bmatrix} 0 \\ Q'_k + \mathcal{K} P_k \\ B_k \end{bmatrix} \right) \cdot \begin{bmatrix} P'_j - \mathcal{K} Q_j \\ Q'_j + \mathcal{K} P_j \\ B'_j \end{bmatrix} \mathrm{d}S \tag{81}$$

$$\mathcal{Q}_{jkl} = EA \int_0^L \left( \frac{EA}{\|\mathbf{r}'\|^2} \begin{bmatrix} \left(Q'_k + \mathcal{K} P_k\right)\left(Q'_l + \mathcal{K} P_l\right) + B'_k B'_l \\ 2\left(P'_k - \mathcal{K} Q_k\right)\left(Q'_l + \mathcal{K} P_l\right) \\ 2\left(P'_k - \mathcal{K} Q_k\right) B'_l \end{bmatrix} \right) \cdot \begin{bmatrix} P'_j - \mathcal{K} Q_j \\ Q'_j + \mathcal{K} P_j \\ B'_j \end{bmatrix} \mathrm{d}S \tag{82}$$

$$\begin{aligned} \mathcal{C}_{jklm} = -\frac{EA}{2} \int_0^L & \begin{bmatrix} 2\left(P'_k - \mathcal{K} Q_k\right)\left[\left(Q'_l + \mathcal{K} P_l\right)\left(Q'_m + \mathcal{K} P_m\right) + B'_l B'_m\right] \\ \left(Q'_k + \mathcal{K} P_k\right)\left[2\left(P'_l - \mathcal{K} Q_l\right)\left(P'_m - \mathcal{K} Q_m\right) - \left(Q'_l + \mathcal{K} P_l\right)\left(Q'_m + \mathcal{K} P_m\right) - B'_l B'_m\right] \\ B'_k\left[2\left(P'_l - \mathcal{K} Q_l\right)\left(P'_m - \mathcal{K} Q_m\right) - \left(Q'_l + \mathcal{K} P_l\right)\left(Q'_m + \mathcal{K} P_m\right) - B'_l B'_m\right] \end{bmatrix} \\ & \cdot \left( \frac{1}{\|\mathbf{r}'\|^3} \begin{bmatrix} P'_j - \mathcal{K} Q_j \\ Q'_j + \mathcal{K} P_j \\ B'_j \end{bmatrix} \right) \mathrm{d}S \end{aligned} \tag{83}$$

# References


[1] Antman, S. (1995). *Nonlinear Problems of Elasticity*. Springer, New York, NY.

[2] Arena, A., Pacitti, A., and Lacarbonara, W. (2016). "Nonlinear response of elastic cables with flexural-torsional stiffness." *International Journal of Solids and Structures*, 87, 267–277.

[3] Benedettini, F. and Rega, G. (1987). "Non-linear dynamics of an elastic cable under planar excitation." *International Journal of Non-linear Mechanics*, 22, 497–509.

[4] Benedettini, F. and Rega, G. (1997). "Experimental investigation of the nonlinear response of a hanging cable. part II: Global analysis." *Nonlinear dynamics*, 14, 119–138.

[5] Benedettini, F., Rega, G., and Alaggio, R. (1995). "Non-linear oscillations of a four-degree-of-freedom model of a suspended cable under multiple internal resonance conditions." *Journal of Sound and Vibrations*, 182, 775–798.

[6] Benedettini, F., Rega, G., and Vestroni, F. (1986). "Modal coupling in the free nonplanar finite motion of an elastic cable." *Meccanica*, 21, 38–46.

[7] Berlioz, A. and Lamarque, C.-H. "A non-linear model for the dynamics of an inclined cable.

[8] Bertrand, C., Acary, V., Lamarque, C.-H., and Ture Savadkoohi, A. (2020a). "A robust and efficient numerical finite element method for cables." *International Journal for Numerical Methods in Engineering*, 121(18), 4157–4186.

[9] Bertrand, C., Plut, C., Savadkoohi, A. T., and Lamarque, C.-H. (2020b). "On the modal response of mobile cables." *Engineering Structures*, 210, 110231.

[10] Crisfield, M. (1997). *Nonlinear Finite Element Analysis of Solid and Structures*. John Wiley and Sons.

[11] Davis, M. (2010). "Lecture notes: Finite difference methods, Course in mathematics and finance, *Imperial College London*.

[12] Ferretti, M., Zulli, D., and Luongo, A. (2019). "A continuum approach to the nonlinear in-plane galloping of shallow flexible cables." *Advances in Mathematical Physics*, 2019.

[13] Floquet, G. (1883). "Sur les équations différentielles linéaires à coefficients périodiques." *Annales Scientifiques de l'École Normale Supérieure*, 12.

[14] Galileo (1638). "Discorsi e dimostrazioni matematiche intorno a due nuove scienze." *Edizione nazionale sotto gli auspicii di sua maesta il re d'Italia*, 7, 186.

[15] Gatulli, V., Lepidi, M., Potenza, F., and di Sabatino, U. (2019). "Modal interactions in the nonlinear dynamics of a beam–cable–beam." *Nonlinear dynamics*, 96, 2547–2566.

[16] Goodey, W. (1961). "On the natural modes and frequencies of a suspended chain." *Quarterly Journal of Mechanics and Applied Mathematics*, 14, 118–127.

[17] Hagedorn, P. and Schäfer (1980). "On non-linear free vibrations of an elastic cable." *International journal of non-linear mechanics*, 15, 333–340.

[18] Huygens, C. (1646). "Correspondance no 21, letter to mersenne, proposition 8." *Dutch academy of sciences*, 36.

[19] Irvine, H. and Caughey, T. (1974). "The linear theory of free vibrations of a suspended cable." *Proceedings of the Royal Society*, 341, 299–315.

[20] Irvine, H. M. (1992). *Cable structures*. Dover, New York OCLC: 831328789.

[21] Kirchoff (1876). *Vorlesungen über Mathematische Physik: Mechanik*. Druck une Verlag von B.G., Leipzig.

[22] Kloppel, K. and Lie, K. (1942). "Die lotrechten Eingenschwingungen des Hangebrucken." *Bauingenieur*, 23, 277.

[23] L., W. and Rega, G. (2010). "Modelling and transient planar dynamics of suspended cables with moving mass." *International Journal of Solids and Structures*, 47, 2733–2744.

[24] Lacarbonara, W. (2013). *Nonlinear Structural Mechanics, The Elastic Cable: From Formulation to Computation*.

[25] Lacarbonara, W. and Pacitti, A. (2008). "Nonlinear modeling of cables with flexural stiffness." *Mathematical problem in Engineering*, 2008.

[26] Lee, C. and Perkins, N. (1992). "Nonlinear oscillations of suspended cables containing a two-to-one internal resonance." *Nonlinear dynamics*, 3, 465–490.

[27] Lee, C. and Perkins, N. (1995). "Three-dimensional oscillations of suspended cables involving simultaneous internal resonance." *Nonlinear dynamics*, 8, 45–63.

[28] Leibniz, G. (1691a). "Solutions to the problem of the catenary, or funicular curve, proposed by M. Jacques Bernoulli." *Acta Eruditorum*.

[29] Leibniz, G. (1691b). "The string whose curve is described by bending under its own weight, and the remarkable resources that can be discovered from it by however many proportional means and logarithms." *Acta Eruditorum*.

[30] Luongo, A., Rega, G., and Vestroni, F. (1982). "Monofrequent oscillations of a non-linear model of a suspended cable." *Journal of sound and vibrations*, 82, 247–259.

[31] Luongo, A., Rega, G., and Vestroni, F. (1984). "Planar non-linear free vibrations of an elastic cable." *International journal of non-linear mechanics*, 19, 39–52.

[32] Marigo, J. J. (2014). *Mécanique des Milieux Continus I*. Paris, École polytechnique, <https://cel.archives-ouvertes.fr/cel-01023392> Lecture notes, HAL-ID: *cel-01023392*.

[33] Pai, P. and Nayfeh, A. (2012). "Fully nonlinear model of cables." *AIAA Journal, Technical notes*, 30.

[34] Pérès, J. (1953). *Mécanique générale*. Masson & Cie.

[35] Perkins, N. (1992). "Modal interactions in the non-linear response of elastic cables under parametric/external excitation." *International journal of Non-linear mechanics*, 27, 233–250.

[36] Pugsley, A. (1949). "On the natural frequencies of suspension chains." *The Quarterly Journal of Mechanics and Applied Mathematics*, 2, 412–418.

[37] Rannie, W. and von Karman, T. (1941). "The failure of the Tacoma narrows bridge." *Federal works agency applications*, VI.

[38] Rega, G. (1996). "Non-linearity, bifurcation and chaos in the finite dynamics of different cable models." *Chaos, Solitons and Fractals*, 7, 1507–1536.

[39] Rega, G. (2004). "Nonlinear vibrations of suspended cables—part i: Modeling and analysis." *Applied Mechanics Reviews*, 57, 443–475.

[40] Rega, G., Alaggio, R., and Benedettini, F. (1997). "Experimental investigation of the nonlinear response of a hanging cable. part I: Local analysis." *Nonlinear dynamics*, 14, 89–117.

[41] Rega, G. and Benedettini, F. (1989). "Planar non-linear oscillations of elastic cables under subharmonic resonance conditions." *Journal of Sound and Vibrations*, 132, 367–381.

[42] Rega, G., Srinil, N., and Alaggio, R. (2008). "Experimental and numerical studies of inclined cables: free and parametrically-forced vibrations." *Journal of theoretical and applied mechanics*, 46, 621–640.

[43] Rega, G., Vestroni, F., and Benedettini, F. (1984). "Parametric analysis of large amplitude free vibrations of a sus pended cable." *International Journal of Solids and Structures*, 20, 95–105.

[44] Rohrs, J. (1851). "On the oscillations o a suspension cable." *Transactions of the Cambridge Philosophical society*, 9, 379–389.

[45] Routh, E. (1868). *Advanced Rigid Dynamics*. Mac Millan, New-York.

[46] Saxon, D. and Cahn, A. (1953). "Modes of vibration of a suspended chain." *The Quarterly Journal of Mechanics and Applied Mathematics*, 6, 273–285.

[47] Simpson, A. (1972). "On the oscillatory motions of translating elestic cables." *20 of Sound and Vibration*, 290, 177–189.

[48] Sofi, A. (2013). "Nonlinear in-plane vibrations of inclined cables carrying moving oscillators." *Journal of Sound and Vibrations*, 332, 1712–1724.

[49] Sofi, A. and Muscolino, G. (2007). "Dynamic analysis of suspended cables carrying moving oscillators." *International Journal of Solids and Structues*, 44, 6725–6743.

[50] Soler, J. (1970). "Dynamic response of single cables with initial sag." *Journal of the Franklin Institute*, 290, 377–387.

[51] Sundararajan, P. and Noah, S. (1997). "Dynamics of forced nonlinear systems using shooting/arc-length continuation methods - application to rotor systems." *ASME, J. Vib. Acoustic*, 119, 9–20.

[52] Triantafyllou, M. (1984). "The dynamics of taut inclined cables." *The Quarterly Journal of Mechanics and Applied Mathematics*, 37(3), 421–440.

[53] Visweswara Rao, G. and Iyengar, R. (1991). "Internal resonance and non-linear response of a cable under periodic excitation." *Journal of Sound and Vibrations*, 149, 25–41.

[54] Warminski, J., Zulli, D., Rega, G., and Latalski, J. (2016). "Revisited modelling and multimodal nonlinear oscillations of a sagged cable under support motion." *Meccanica*, 51, 2541–2575.

[55] Wu, Q., Takahashi, K., and Nakamura, S. (2005). "Formulae for frequencies and modes of in-plane vibrations of small-sag inclined cables." *Journal of Sound and Vibrations*, 279, 1155–1169.